Supporting Information

Strain in Catalysis: Rationalizing Material, Adsorbate, and Site Susceptibilities to Biaxial Lattice Strain

Cheng Zeng[†], Tuhina Adit Maark[†,‡], and Andrew A. Peterson[*]

School of Engineering, Brown University, Providence, Rhode Island, 02912, United States.
**Corresponding author: Email: andrew_peterson@brown.edu, Tel: +1 401-863-2153*
[‡]Current address: Department of Physics, Indian Institute of Technology Madras, Chennai 600036, India.
[†]These authors contribute equally to this work.

This Supporting Information (SI) includes the correlation between $d\bar{\varepsilon}_{\mathrm{d}}/de_{x,y}$ and $dW_{\mathrm{d}}/de_{\mathrm{x,y}}$, a derivation of susceptibility of d–d coupling matrix element to equi-biaxial strain, eigenforce analysis for an outlier of site dependency, scaling relations for the other two pairs of adsorbates OH vs O and CH_x vs C , and the detailed comparisons between eigenforce predictions and DFT values on three example surfaces.

S-1 Correlation between $d\bar{\varepsilon}_{\mathrm{d}}/de_{x,y}$ and $dW_{\mathrm{d}}/de_{\mathrm{x,y}}$

A weak linear correlation between $d\bar{\varepsilon}_{\mathrm{d}}/de_{x,y}$ and $dW_{\mathrm{d}}/de_{\mathrm{x,y}}$ was identified (R^2=0.47).

S-2 Susceptibility of d-d coupling matrix element to strain

In this work, a strong correlation between susceptibilities of d band width and binding energy to strain was observed. d band width of a surface atom i is proportional to the sum of d-d band coupling matrix element of the atom interacting with its nearest neighbors [1]. It takes the form:

$$V_{\mathrm{i}} = \frac{\eta_{ddm}\hbar^2}{m}\sum_{j=1}^{NN}\frac{[r_{\mathrm{d}}^{(i)}r_{\mathrm{d}}^{(j)}]^{3/2}}{d_{ij}^5}$$

We shall show the susceptibility of matrix element to strain. We first consider the change of V_{i}, induced by an equi-biaxial strain. We denote the Poisson's ratio for response in the direction normal to the surface as ν_z, and components of distance vector between atom i and its nearest neighbor atom j on x, y and z dimension are represented by $d_{ij,x}$, $d_{ij,y}$, and $d_{ij,z}$, respectively. With an equi-biaxial strain ϵ_{b}, V_i becomes

$$V_{\mathrm{i}}(\epsilon=\epsilon_{\mathrm{b}}) = \frac{\eta_{ddm}\hbar^2}{m}\sum_{j=1}^{NN}\frac{r_{\mathrm{d}}^3}{\left(\sqrt{(1+\epsilon_{\mathrm{b}})^2d_{ij,x}^2+(1+\epsilon_{\mathrm{b}})^2d_{ij,y}^2+(1-\nu_z\epsilon_{\mathrm{b}})^2d_{ij,z}^2}\right)^5}$$

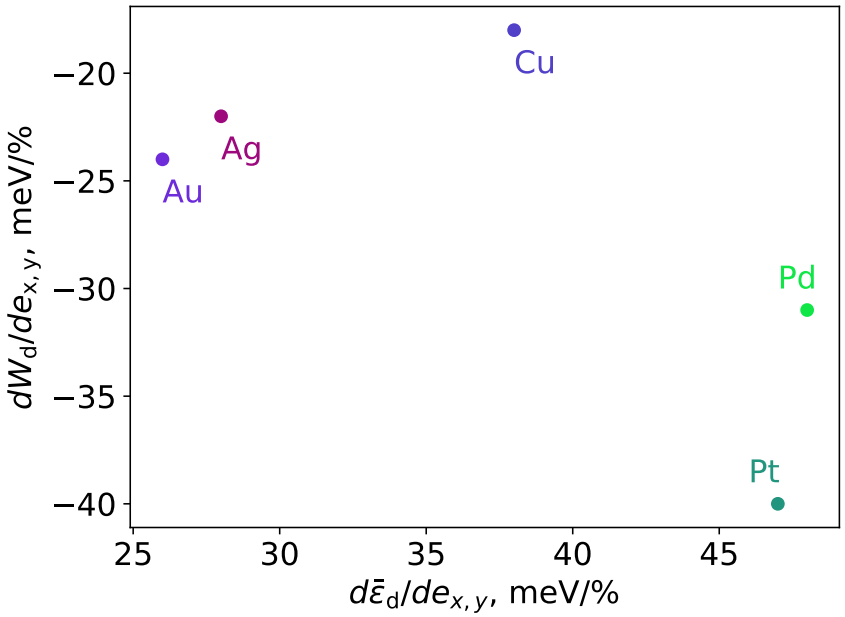

Figure S1: The correlation between $d\bar{\varepsilon}_{\mathrm{d}}/de_{x,y}$ and $dW_{\mathrm{d}}/de_{\mathrm{x,y}}$ of a clean fcc(111) surface across five metals.

Extracting $(1+\epsilon_{\mathrm{b}})^2$ from the denominator, we have:

$$V_{\mathrm{i}}(\epsilon=\epsilon_{\mathrm{b}}) = \frac{\eta_{ddm}\hbar^2}{m}\sum_{j=1}^{NN}\frac{r_{\mathrm{d}}^3}{(1+\epsilon_{\mathrm{b}})^5\left(\sqrt{d_{ij,x}^2+d_{ij,y}^2+d_{ij,z}^2+\left(\frac{(1-\nu_z\epsilon_{\mathrm{b}})^2}{(1+\epsilon_{\mathrm{b}})^2}-1\right)d_{ij,z}^2}\right)^5}$$

Since $\epsilon_{\mathrm{b}} \ll 1$, it implies $(1-\nu_z\epsilon_{\mathrm{b}})^2 \approx 1-2\nu_z\epsilon_{\mathrm{b}}$ and $(1+\epsilon_{\mathrm{b}})^2 \approx 1+2\epsilon_{\mathrm{b}}$. $V_{\mathrm{i}}(\epsilon=\epsilon_{\mathrm{b}})$ then reads as:

$$V_{\mathrm{i}}(\epsilon=\epsilon_{\mathrm{b}}) \approx \frac{\eta_{ddm}\hbar^2}{m}\sum_{j=1}^{NN}\frac{r_{\mathrm{d}}^3}{(1+\epsilon_{\mathrm{b}})^5\left(\sqrt{d_{ij}^2-\frac{2(1+\nu_z)\epsilon_{\mathrm{b}}}{(1+2\epsilon_{\mathrm{b}})}d_{ij,z}^2}\right)^5}$$

Susceptibility of the matrix element (χ_{V_i}) is defined as:

$$\chi_{V_i} = \frac{V_{\mathrm{i}}(\epsilon=\epsilon_{\mathrm{b}})-V_{\mathrm{i}}(\epsilon=0)}{\epsilon_{\mathrm{b}}-0}$$

As ϵ_{b} is small, we shall approximate the susceptibility by taking the derivative of $V_{\mathrm{i}}(\epsilon=\epsilon_{\mathrm{b}})$ with respect to ϵ_{b}, and the susceptibility is then given by the derivative at $\epsilon_{\mathrm{b}}=0$. We write:

$$\chi_{V_i} \approx -\frac{5\eta_{ddm}\hbar^2}{m}\sum_{j=1}^{NN}\left(\frac{r_{\mathrm{d}}^3}{d_{ij}^5}\left[1-\frac{(1+\nu_z)d_{ij,z}^2}{d_{ij}^2}\right]\right)$$

For a atom i on the top layer of a fcc(111) surface, it has 9 nearest neighbors, 6 on the top layer and 3 on the second layer. For atoms in the top layer, we have $d_{ij,z}=0$, and for atoms in the second

Table S1: Poisson's ration in the direction normal to the surface when an equi-biaxial strain is applied. Here $\nu_{z,t}$, $\nu_{z,c}$ and $\bar{\nu}_z$ are the Poisson's ratio estimated using tensile strain $+2.0\%$, using compressive strain -2.0%, and taking the average, respectively.

Surfaces	$\nu_{z,t}$	$\nu_{z,c}$	$\bar{\nu}_z$
Cu(111)	0.89	0.92	0.91
Pd(111)	0.95	0.89	0.92
Ag(111)	0.79	1.24	1.01
Pt(111)	1.05	1.11	1.08
Au(111)	1.47	1.54	1.51

layer, simple geometry analysis gives $d_{ij,z}^2/d_{ij}^2 = 2/3$. One should note that d_{ij} is the interatomic distance without strain, and it is the same for all nearest neighbors (atom js). Plugging expressions for $d_{ij,z}$ for the above two types of neighbors, the susceptibility is simplified:

$$\begin{aligned}\chi_{V_i} =& -\frac{5\eta_{ddm}\hbar^2}{m}\left(6\times\frac{r_{\mathrm{d}}^3}{d_{ij}^5}+3\times\left(1-\frac{2(1+\nu_z)}{3}\right)\frac{r_{\mathrm{d}}^3}{d_{ij}^5}\right)\\ =& -\frac{5\eta_{ddm}\hbar^2}{m}\times\frac{(7-2\nu_z)r_{\mathrm{d}}^3}{d_{ij}^5}\end{aligned}$$

Here $\frac{5\eta_{ddm}\hbar^2}{m}$ is a constant across all metal surfaces and $d_{ij}\propto a$, where a is the lattice constant of a bulk cell. Therefore, the d band width susceptibility is related to the electronic factor r_d and geometric factor d in the form of:

$$\chi_{W_d^{(i)}}\propto\chi_{V_i}\propto\frac{(2\nu_z-7)r_{\mathrm{d}}^3}{d_{ij}^5}\propto\frac{(2\nu_z-7)r_{\mathrm{d}}^3}{a^5}$$

The proportionality requires the Poisson's ratio in the z direction when an in-plane bi-axial strain is applied. In this study, it is approximated by the change of relative interlayer z distance between the top and second layer subject to the strain. We calculate the Poisson's ratios with tensile strain $+2.0\%$ and compressive strain -2.0%, and we use the average in Figure 5. The estimated values of Poisson's ratios are shown in Table. S1.

S-3 Eigenforce analysis for outliers of site dependency: A case study of O on Pt

A few outliers can be identified on Figure 5, such as O on Pt and OH on Cu. A rigorous understanding requires a detailed analysis of the electronic structure change due to strain, which is out of the scope for this study. In the eigenforce framework, atomic forces, resulting from electron structures based on the Hellmann–Feymann theorem, could offer a direct qualitative explanation for the unexpected trend. [2–4] We use the O on Pt as the example, and we consider the adsorption on two sites (ontop and hcp), as shown in Figure 5. The eigenforces on the most impactful surface atoms are shown in Figure S2.

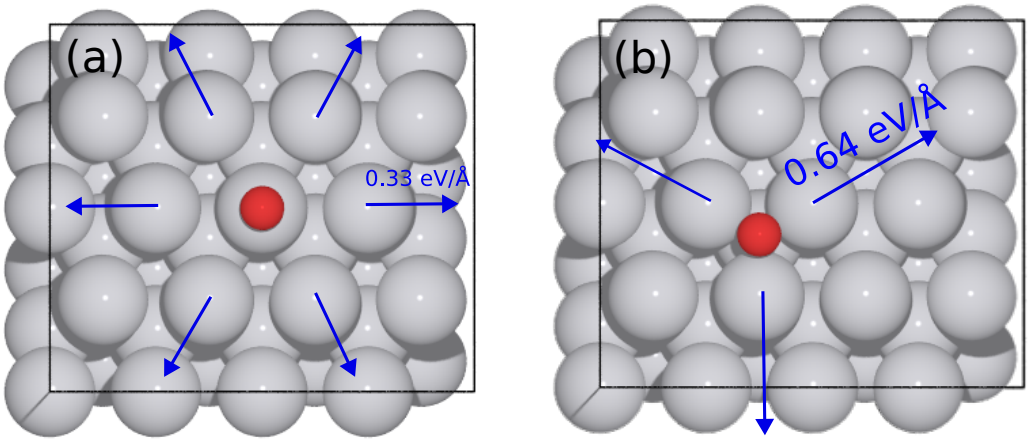

Figure S2: Eigenforce analysis for the site dependency of O on Pt. Two adsorption sites are compared: ontop (a) and hcp (b) site.

S-4 Scaling relationships of OH_x vs O and CH_x vs C

Figure S3 shows the linear scaling relationships fitted on unstrained surfaces and variations of the binding energy due to strain with respect to the OH vs O pair. The sites of OH on Cu, Pd, Ag, Pt and Au are fcc, bridge, fcc, ontop and fcc, respectively. And O is bonded to an fcc site for all surfaces. Based on the geometry analysis, the slopes of coordination numbers are 3/3, 2/3, 3/3, 1/3, 2/3 for respective Cu, Pd, Ag, Pt and Au, which are in accordance with calculated slopes of susceptibilities 1.10 for Cu, 0.67 for Pd, 1.24 for Ag, 0.32 for Pt, and 1.63 for Au.

Figure S4 shows the linear scaling relationships fitted on unstrained surfaces and variations of the binding energy due to strain with respect to the CH_x vs C pairs. The simple logic using coordination numbers cannot be easily applied to CH_x vs C pairs. For example, CH_2 sits on a bridge site on Pd and Pt, hence the slopes of coordination numbers are 2/3. Yet the slopes of susceptibilities are 0.25 and 0.05 on Pd and Pt, respectively, much smaller than that predicted the geometry analysis. We attribute the uniqueness of CH_x vs C pairs to the high susceptibility of C and relatively small susceptibilities of CH_x. Nevertheless, the geometry logic is qualitatively accurate for CH_x vs C pairs. On both Pd and Pt, C, CH, CH_2 and CH_3 favor respective fcc, fcc, bridge and ontop sites. Therefore, slopes of susceptibilities are predicted to be in the order of CH vs C > CH_2 vs C > CH_3, which agree well with calculated values.

S-5 Eigenforce predictions versus DFT calculated values

Figure S5 indicates that the model tends to predict better for Cu(111) and Pd(111) surfaces, with a MAE of respective 0.004 and 0.010 eV/Å, while larger but systematic deviations (over-predictions) are found for adsorbates on the Pt(111) surface, resulting in a MAE of 0.024 eV/Å. Nevertheless, trends of strain-induced binding energy changes are well represented by the eigenforce predictions for all cases.

Figure S6 shows the eigenforce predicted strain susceptibilities versus the DFT results on rigid surfaces, excluding the effect of surface relaxation. It demonstrates that the large error for Pt in Figure 8 originates from surface relaxation.

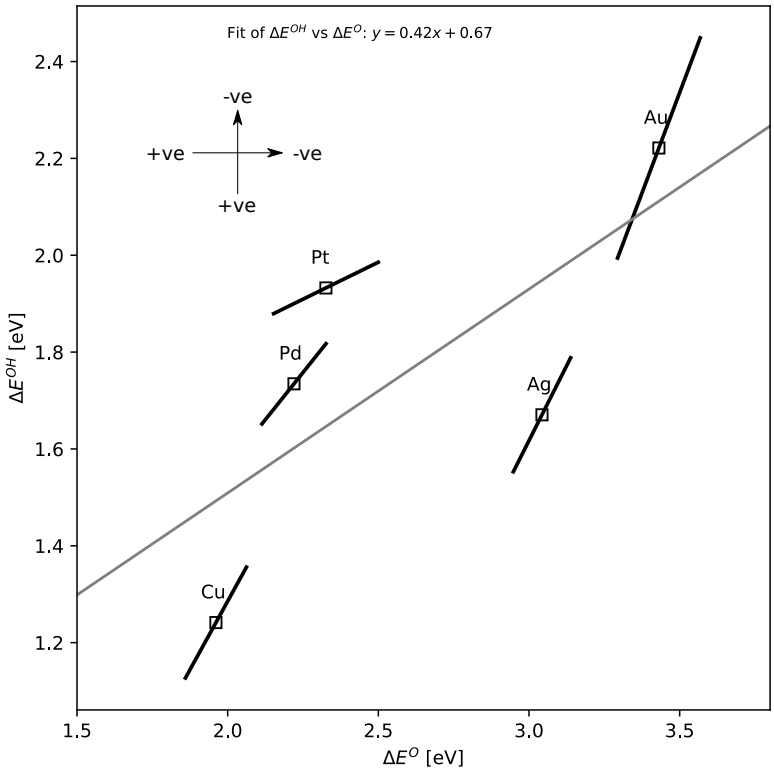

Figure S3: ΔE^{OH} vs ΔE^{O} variation for for $\pm 2.0\%$ biaxially strained Cu, Pd, Ag, Pt and Au(111) surfaces and the slopes or linear scaling constants fitted using the results without strain depicted as grey lines. The data points corresponding to pair adsorbates of (OH, O) are represented by black squares. The strain induced changes for (OH, O) are plotted by black solid lines. The arrows give the sign and direction of applied biaxial strain.

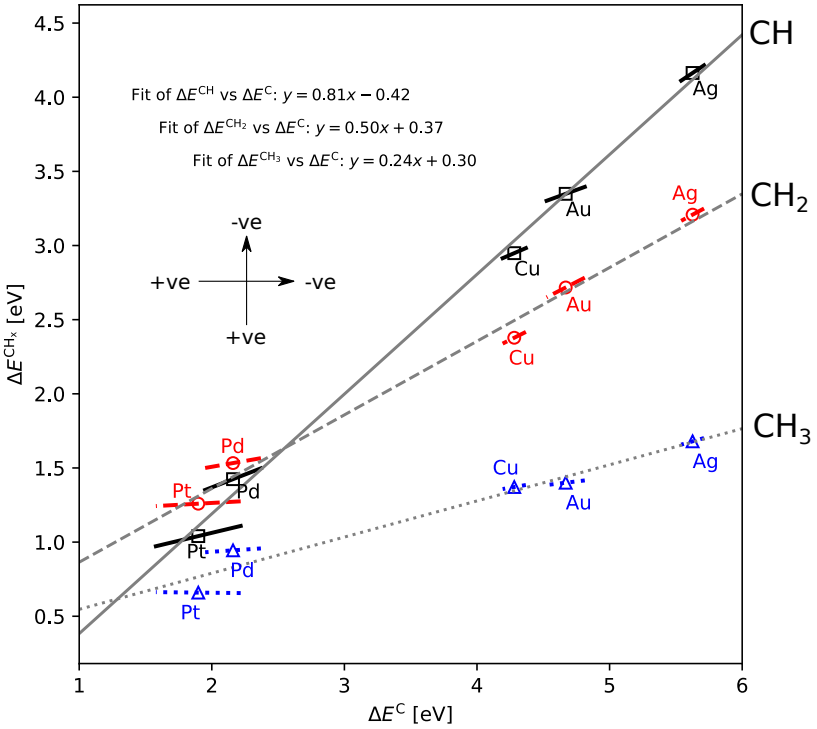

Figure S4: ΔE^{CH_x} vs ΔE^{C} variation for for $\pm 2.0\%$ biaxially strained Cu, Pd, Ag, Pt and Au(111) surfaces and the slopes or linear scaling constants fitted using the results without strain depicted as grey lines. The data points corresponding to pair adsorbates of (CH_3, C), (CH_2, C) and (CH, C) are represented by blue triangles, red circles and black squares, respectively. The strain induced changes for (CH_3, C), (CH_2, C) and (CH, C) are plotted by the blue dotted, red dashed and black solid lines, respectively. The arrows give the sign and direction of applied biaxial strain.

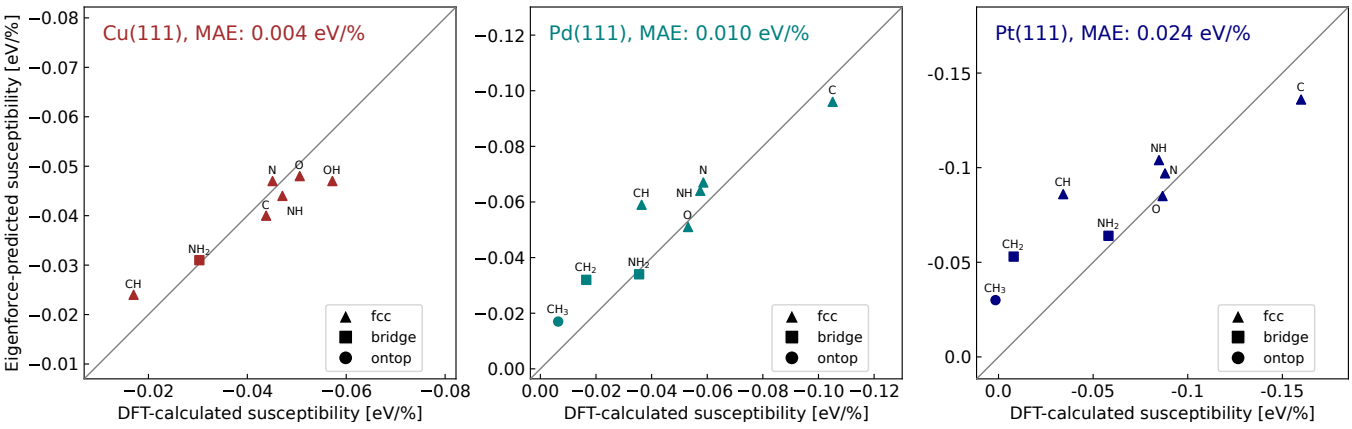

Figure S5: Eigenforce model predicted strain susceptibilities. Adsorbates are labeled next to scatter points. Adsorption sites are indicated by marker shapes.

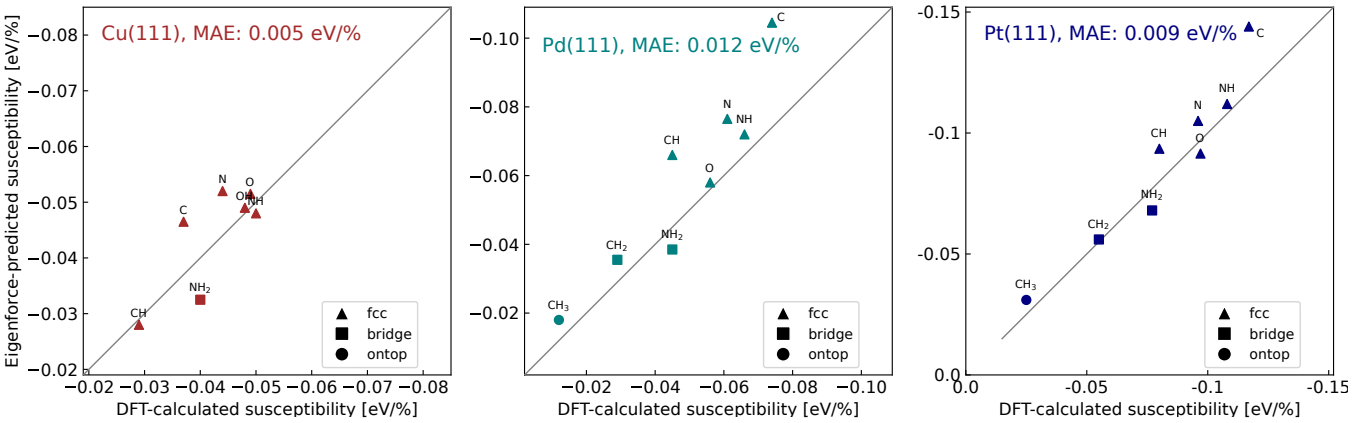

Figure S6: Eigenforce model predicted strain susceptibilities versus DFT calculated values on rigid surfaces.

References

[1] Kitchin, J. R.; Nørskov, J. K.; Barteau, M. A.; Chen, J. G. *Role of strain and ligand effects in the modification of the electronic and chemical properties of bimetallic surfaces. Phys. Rev. Lett.* **2004**, *95*, 156801(1–4).

[2] Khorshidi, A.; Violet, J.; Hashemi, J.; Peterson, A. A. *How strain can break the scaling relations of catalysis. Nature Catalysis* **2018**, *1*, 263–268.

[3] Sharma, S.; Zeng, C.; Peterson, A. A. *Face-centered tetragonal (FCT) Fe and Co alloys of Pt as catalysts for the oxygen reduction reaction (ORR): A DFT study. The Journal of Chemical Physics* **2019**, *150*, 041704.

[4] Feynman, R. P. *Forces in molecules. Physical Review* **1939**, *56*, 340–343.